Development of Laser Machined Metamaterial Optical Elements for Cosmic Microwave Background Observations

Joseph E. Golec

Advisor: Jeffrey J. McMahon

2016-2017

Submitted to the University of Michigan in partial fulfillment of graduation requirements
for Honors in the degree of Bachelor of Science in Physics

Abstract

The Cosmic Microwave Background (CMB) is the earliest observable radiation in the universe and observation of the CMB gives an insight into the physics of its earliest moments. The Atacama Cosmology Telescope (ACT) observes the CMB in the hope to answer questions about inflation and large scale structure of the universe. To do this, precision optical techniques and equipment must be utilized. One of the optical features of ACT is the sub-wavelength features machined in its lenses that act as an anti-reflection coating. We present a new laser ablation technique for creating these AR coatings as well as future applications for laser machining in regards to ACT and other optical experiments.

Contents

1 Acknowledgements

There are a lot of people I would like to thank for the opportunity to do the work that I have done here. First, I would like to thank Professor Jeff McMahon. Four years ago, Jeff told me that it would be a pleasure to have me work in his lab, but I think after these four years I can say that the pleasure is all mine and I don't think my undergraduate experience would have been the same without your guidance. I would like to also thank Charles Munson, Kevin Coughlin, Fletcher Boone, and Rahul Datta for all the advice that they have given me. I don't think I would know where anything was in the lab or how to do basic laboratory functions, like run a vacuum pump or solder, without them. Lastly, I would like to thank all of my peers who have worked on this project before me, with me, and who will most assuredly improve my project in the future.

2 Motivation

It is not hard to believe that the the study of the stars and the universe began with the ancients who gazed at the night sky wondering what the heavens contained. It was not so long ago that Galileo and Copernicus used their telescopes to observe celestial bodies. The modern field of cosmology began in the early 1900s with Einstein's theory of general relativity and observational cosmology began soon after that. Today, we use much more sophisticated technology than Galileo and Copernicus, however the concept is much the same. We pick points in space to observe, we take data, and then we analyze that data to understand more about our universe.

One of the most fascinating cosmological objects to observe is the Cosmic Microwave Background (CMB). It is fascinating because of the cosmological parameters that we can measure from it. These parameters are then compared to theoretical models, and together they help us better understand the universe that we live in. Thus, more sophisticated and precise measurements of the CMB yield an even better understanding of the universe. This drive for more accurate measurement is the reason for the development of the technology described in this thesis. CMB observations have many systematic parameters that effect the quality of the measurement. One of the largest contributions to the error in measurements are foreground emissions from galactic dust. These foreground emissions manifest in the high frequency bands of observation and the results from BICEP2 show that dust emission is not negligible [10]. This result means that we need a better understanding of the foregrounds in the low terahertz bands. To this end, I developed anti-reflection (AR) coatings that improve the throughput of the optical elements that operate at those frequencies. This thesis discusses the geometry and fabrication of these AR coatings using new techniques of laser ablation.

3 The Cosmic Microwave Background

The CMB was discovered in 1964 by Penzias and Wilson, who were awarded the Nobel Prize in 1978 for their discovery. Since then, the CMB has been the tool that cosmologists use to test theories and models of the universe.

When the universe was first created, the matter that made it up was too energetic to form atoms and thus was ionized. This means that electrons were not bound to the nucleus and were free in space. Due to these free electrons, photons could not propagate due to Compton Scattering and thus the universe was opaque. During the epoch of recombination, when the energy of the universe lowered enough to bind the electrons to the nucleus, photons could freely propagate through the universe, but not without scattering off free electrons one last time. This happened around 380,000 years after the big bang when the temperature of the universe was around 3000 kelvin. These photons that interact one last time make up the CMB that we observe.

3.1 CMB Observation

Thanks to experiments like the Cosmic Background Explorer (COBE) we know the temperature of the CMB today very precisely. Using the FIRAS instrument, COBE measured the spectrum of the CMB to be that of a perfect black body radiating at 2.726 ± 0.010 K [1] and using the DMR instrument, COBE measured the anisotropies in the CMB to be one part in 10^5 [2]. These measurements earned Smoot and Mather the Nobel Prize in 2006.

The result that the temperature of the CMB was uniform was validation for the so called cosmological principal, that the universe is homogeneous and isotropic. It also caused a greater interest in the anisotropies of the CMB because the study of the fluctuations in the temperature may yield results that have implications for large scale structure of the

universe. This lead to another satellite mission, the Wilkinson Microwave Anisotropy Probe (WMAP). WMAP measured the anisotropies of the CMB more accurately and on greater angular scales than COBE. [3]

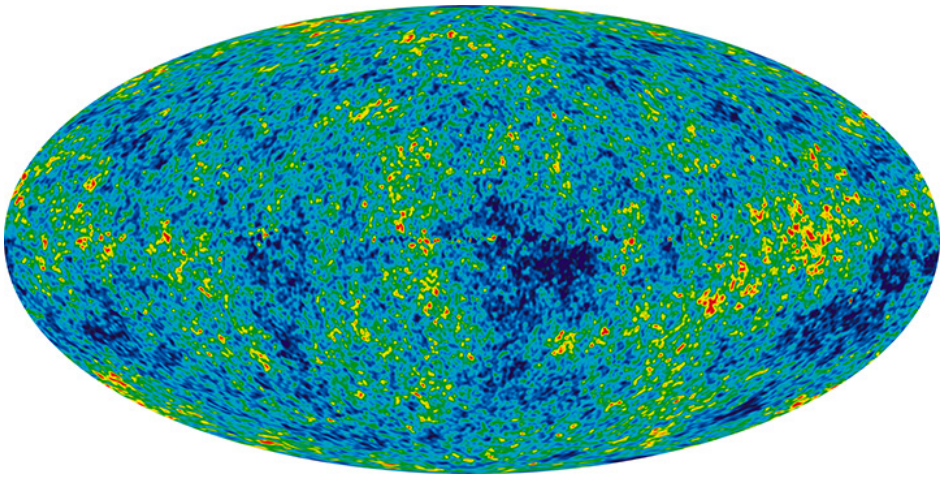

Figure 1: WMAP nine year map of the microwave sky.

After WMAP came the Planck Satellite which had a better angular resolution than WMAP and further measured the anisotropies of the CMB. Plank also observed the CMB in nine frequency bands as opposed to WMAP's five bands. This meant that Planck had better foreground measurements and could better filter anomalies from their data. From these satellite missions, better fits to cosmological models were found and better constraints on the parameters of the ΛCDM model were proposed.

COBE, WMAP, and Planck were all satellite missions to measure the CMB, but there have been numerous ground and balloon based experiments that measure it. While the atmosphere is a problem to these ground based experiments it was found to be an issue that could be systematically dealt with and thus ground based experiments are a good compliment to the space based ones. The atmosphere contributes noise to measurements, so the ground based experiments are located in areas where the atmosphere is dry and thin like Antarctica and the Atacama Desert in Chile. These experiments are actually advantageous to space missions in a way; they permit researchers to build bigger telescopes that would be

unfeasible to send into space as well as allow researchers to improve the technology of the experiments as those advances become available.

3.1.1 ACT

The Atacama Cosmology Telescope (ACT) is one of the CMB experiments located in the Atacama Desert in Chile. ACT was designed to be a high-ell experiment which had a resolution of about one arcminute. This resolution was accomplish by a six meter primary mirror. ACT originally observed in three frequency bands, 145, 215, and 280 GHz using a focal plane array of TES bolometers. These bands were observed because of one of ACT's goals, observing the Sunyaev-Zel'dovich (SZ) effect, needs a null temperature calibration at 217 GHz and because observing in multiple bands allows for foreground characterization of anisotropies caused by sources other than the CMB such as dust and point sources.

In 2010, ACT released its arcminute resolution measurements of the CMB. Within this measurement, uncatalogued point sources were found as well as signatures that are characteristic of the SZ effect. [4] From the initial data, ACT was also able to detect evidence of gravitational lensing.

ACT was upgraded in 2013 to ACTPol. The goal of ACTPol was to measure the temperature and polarization anisotropies at high-ell. These measurements probe the spectral index of inflation, the primordial helium abundance, and the neutrino mass sum. Another science goal of ACTPol is to study gravitational lensing of the CMB and B-mode polarizations. This goal allows us to study the effect of dark energy at earlier times in our universe's history. Lastly, ACTPol made the catteloging of clusters via the SZ effect a goal. This goal leads to the study of early large scale structure formation. These science goals mean that the telescope needed a hardware upgrade to be polarization sensitive, so a new multi-chroic polarimeters were added in the 150 and 220 GHz band. Another change from ACT to ACTPol

was the addition of an anti-reflection (AR) coating on the lenses of the telescope.

This anti-reflection coating consists of cutting sub-wavelength structures into the lenses to increase the transmission in the observing bands. This AR coating is made by cutting stepped pyramid like structures into the silicon with a dicing saw. By manipulating parameters, such as the pitch of these structures, one can define which frequency band is more transmissive.

ACTPol is currently being upgraded to AdvACTPol. The goal of AdvACT is to upgrade the ACTPol experiment by filling the entire focal plane with multi-chroic detectors and to add a rotating Half-Wave Plate (HWP). The addition of more multi-chroic arrays allows again for a better understanding of the foregrounds that spoil polarization detection. The addition of the HWP allows ACT to modulate the polarization signal that it receives so that it can factor out the polarization from the instrumentation itself.

With these improvements, AdvACT seeks to halve the uncertainties of the basic cosmological parameters of the ΛCDM model, map nearly half of the microwave sky, and achieve a variance-limited measurement of the primordial CMB polarization out to ℓ=2000. [5] The last of the previously mentioned science goals is of the most interest as accurate measurement of primordial CMB polarization helps us best understand the theorized inflationary period of the universe.

3.2 Future CMB Experiments

The next generation of CMB experiments will be a ground based telescope named the Simons Observatory and various balloon based experiments. All of the future experiments will claim to put lower bounds on cosmological parameters and in order to make these claims they will need to understand the dust foregrounds that were previously discussed. To do

this, all future experiments will include frequency bands in the near or low terahertz. This means that optical elements will need to be developed to increase the throughput of the system in these bands. That is why I have developed the AR coatings that are going to be discussed next.

4 Metamaterial Anti-Reflection Coatings

A large part of the success of the ACT experiment is increasing the throughput of the system by developing an Anti-Reflection (AR) coating for silicon lenses and HWP. Effective AR coatings have been developed by cutting sub-wavelength features into the surface of the material being coated. This process is described thoroughly in Datta et al [7]. Essentially, a large silicon dicing saw is used to cut micron sized features into a silicon lens or wafer. These features produce an effective index of refraction on the surface of the silicon that acts as an AR coating. Since the features are cut into the material itself it is extremely applicable in systems where thermal contraction is an issue.

The geometry of these cuts is that of stacked rectangular prisms of changing width, lengths, and heights.

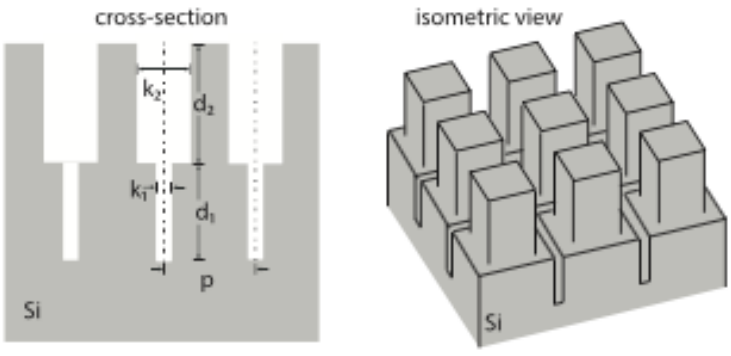

Figure 2: The geometry of ACTPol's AR coating.[7]

This coating is machined carefully and over the course of weeks. The resulting efficiently is summarized in Datta et al. In the band of 120 to 165 GHz the reflectance is below 0.01%. Those results are much to be desired, therefor we set out to try and replicated that geometry with our laser machining process.

For the near terahertz band the stepped pyramid design becomes less effective, so we looked for a different geometry. There is a different geometry that cannot be accomplish via a dicing saw, and that is an array of cones.

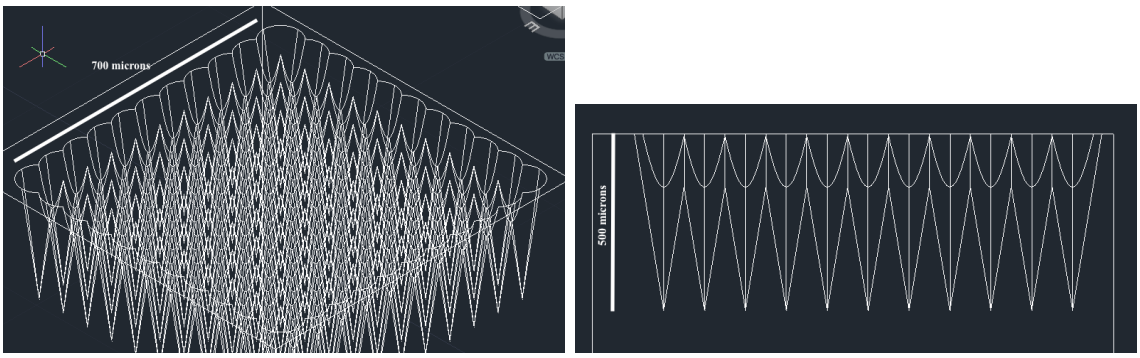

Figure 3: The conical geometry. Left Isometric view. Right cross section.

The geometry in Figure 3 is difficult to achieve in silicon via mechanical means due to the nature of silicon to chip and crack from drilling, so it has not been used as an AR coating. Since the natural profile of a focused laser beam is similar to a cone, we made it a goal to test this geometry. To see how efficient it can be we modeled it in a program called HFSS. This program allows the user to test the throughput of a model array of geometries. The following plot is the HFSS simulation results for an array of cones of diameter 90 microns, pitch of 75 microns, and depth 500 microns.

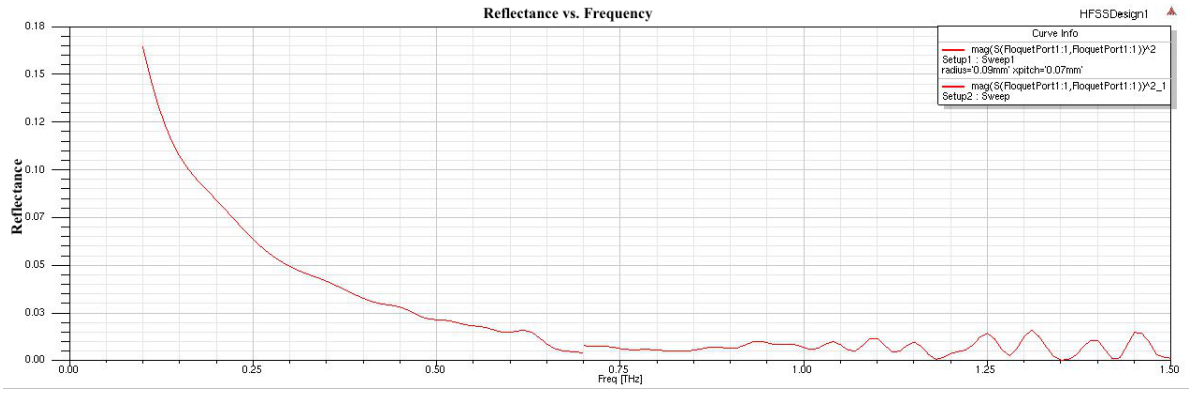

Figure 4: Reflectance versus frequency.

My simulation shows that the cone array geometry is an effective AR coating in the low terahertz regime, which is a much higher frequency than the silicon diced AR coating. This means that we can increase the throughput of optical systems in a frequency band that we have not been able to improve in the past with the previous AR geometries. Thus we selected to try and produce this geometry with our laser.

5 Fabrication of Metamaterial Optics

In order to achieve the modeled geometries, an innovative laser machining system had to be developed. To this end, I designed and built the laser machining system shown below. It took approximately two months to assemble and a little longer than that to power up the laser for the first time. As with any project that involves a high powered class four laser, safety was a concern. With that in mind we designed a box that completely contains the laser machining system, and is complete with safety interlocks that I installed to ensure that if the box was ever opened, the shutter to the laser closes and no one could possibly be harmed. With these safety precautions we have effectively turned a class four laser threat into a class one system.

Figure 5: The machining system with the doors to the laser closed.

The laser is mounted on a commercial (Areotech) three stage system. These stages have micron order accuracy, can move at a maximum speed of around a meter a second, and have a settle time on the order of microseconds. This combination allows us to have quick and precise control which is required for micron order machining. They are controlled using Areotech controller code from a computer attached to the system.

The laser itself is mounted to the z-stage which is in turn mounted to the y-stage. The sample to be cut with the laser would be mounted to the x-stage. This three stage configuration gives us three degrees of freedom to cut in; x and y freedom allows us to define where on the sample our beam is located and the z direction allows us to focus the spot size of our beam on our sample. The x-stage has a maximum limit of travel of 650 mm and the y-stage has a maximum limit of travel of 630 mm. Thus we can comfortably machine a sample that is around 400 square millimeters.

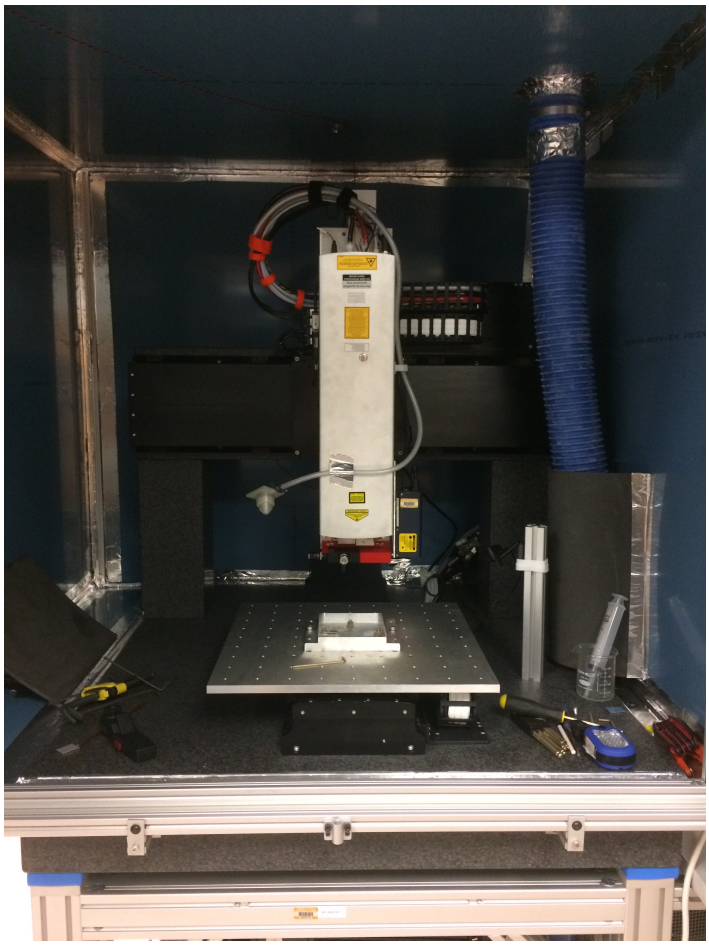

Figure 6: The machining system with the laser mounted.

We use lenses of a variety of focal lengths to focus our beam depending on what we want to accomplish. The advantage to using different lenses is we achieve different beam profile at the focus. In many cases, we need to know the profile of the laser beam so we know how our cut is going to look. The parameters that we care about are the waist or diameter of the beam at the focal length, and the Rayleigh length of the beam. The waist is important because it is the resolution that we a limited to by our cuts. The Rayleigh length is an important parameter because it will determine how the beam spreads out over a certain height. For example a short Rayleigh length means that the spot size of the beam spreads out quickly and thus will create sloped walls. Whereas a large Rayleigh length means that we maintain the focal spot size for a greater range of heights and thus will have straighter walls. The straightness of the cut walls will be important depending on what features are

trying to be achieved. The diameter of the beam waist at the focus is given by

$$D = 2\omega_0 \simeq \frac{4\lambda}{\pi\Theta_{Div}}$$

where λ is the wavelength of the laser, in our case 0.350 microns, and Θ_{Div} is related to the focal length of the lens being used to focus the beam. This relation is given by simple triginometry,

$$\Theta_{Div} = 2\arctan\frac{3.5/2}{f}$$

where f is the focal length of the lens in millimeters and 3.5/2 mm is the waist of the collimated beam emitted by the laser. We can then find the Rayleigh length of the focused beams from

$$z_r = \frac{\pi\omega_0^2}{\lambda}$$

this gives us the distance from the focus where the diameter of the spot size increases by a factor of $\sqrt{2}$. Therefor the optimal distance from the sample to the lens is the focal length plus or minus the Rayleigh length. The following table summarizes these parameters of the lenses that we use.

Focal Length (mm)	**Waist** (μm)	**Rayleigh Length**(μm)
15	0.97	8.377
49	3.17	88.67
50	3.23	92.32
100	6.46	369.055

Table 1: Optical parameters of the lenses that we used.

The two extreme focal lengths, 15 mm and 100 mm, were tested heavily to see their contrasting properties.

5.1 Laser Parameters

We are using a Talon 355-20 laser system. This system is diode pumped and q-switched. The maximum power output of this laser is around 20 Watts but we operate it at around 13 Watts as measured by the laser's GUI. [6] We can control the power output of the laser by changing the repetition frequency (QSW) of the laser. We tested this parameter space and plotted the results. This particular test was at a constant EPRF, which is a parameter that regulates the energy limit of the system.

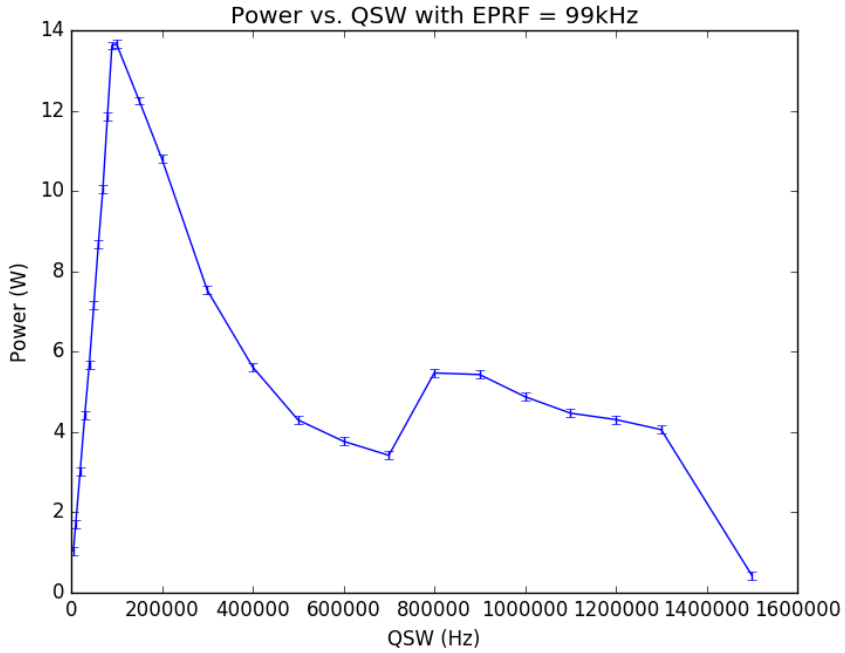

Figure 7: Laser power versus repetition rate.

We usually operated the laser at a QSW of 100 kHz which, on average gave generated an output power of around 13 Watts. At that power, this gives a fluence of 10 MW per cm^2 for the 100 mm focal length lens and 439 MW per cm^2 for the 15 mm focal length lens.

5.2 Non-Contact Laser Metrology

To image any features that we create on a sample, we used methods ranging from imaging with a microscope to taking pictures with a camera with a high zoom lens. These work for a rough image of what the features look like, but to get a more accurate measurement we used a ConoPoint laser distance sensor. This sensor works by shining a laser beam on a surface and then interfering this incident laser beam with the reflected beam off the surface. The sensor then measures the interference fringes to calculate the distance from the probe to the surface. Using the distance measurements we can create an image of the surface.

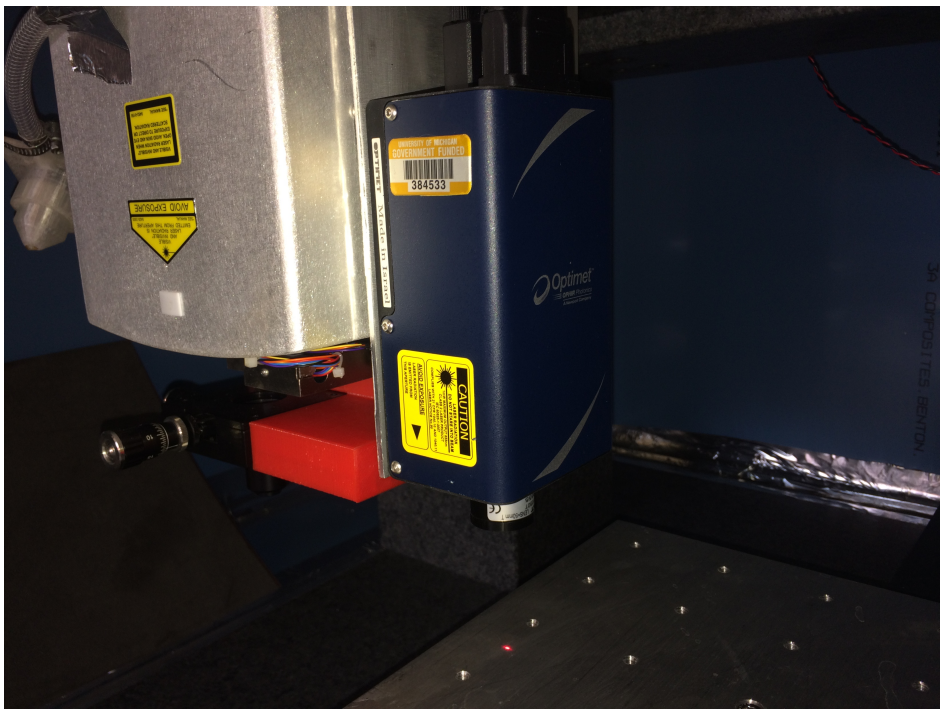

Figure 8: ConoPoint sensor mounted to the laser.

6 Prototype Metamaterial Optics

With these preliminaries discussed, we can now cover the actual tests of machining different materials. This machining was performed over the course of several months and the results are presented here. We mainly focused on the machining of silicon, but a few other materials were experimented with as well; notably alumina, glass, and acrylic. There were many tests performed on these materials, but the tests that have the most important applications are those that apply to the AR coatings previously discussed. These AR coating geometries were only cut in silicon and alumina.

After some initial cutting on silicon we discovered that there was a white substance that was being redeposited in the surface of the silicon. This substance could not be washed off with water or weak solvents such as isopropanol or acetone. To eliminate this redeposited material, we placed a layer of water on top of the silicon when we cut it. This seemed to eliminate the redeposited material completely, but at the cost of attenuating the laser's power. However, this attenuation effect did not drastically reduce the amount of material that we ablated away, so we did not consider it a large factor in the overall machining process.

6.1 Rectangular Geometry

We first tried to cut the rectangular AR coating into silicon. This was accomplished by rastering the beam across the surface of the silicon with 21 micron spacing for a 300 micron patch, skipping a 300 micron patch, and then repeating the rastering process. This was done in the y direction first and then repeated in the x direction. This process was introduced to us by Matsumura et al [8]. We found the best results of this method by using the 100 mm focal length lens, a scanning speed of around 10 mm/sec, and around 50 passes over the same area.

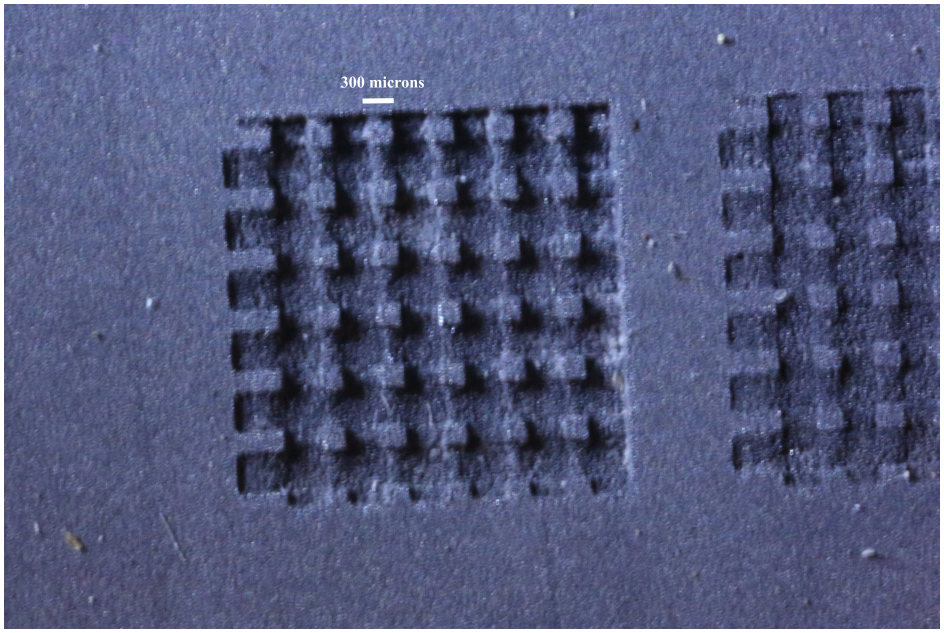

Figure 9: Rectangular AR coating.

Preliminary results show that the width of the beam itself plays a role in the kerf of the cuts made. This is seen in the discrepancy between the size of the ablated and non-ablated regions. They should be the same width, but measurement shows that the ablated region is slightly wider than the non-ablated region. Another interesting feature is an artifact from the scanning method; certain areas only get passed over twice as much with the laser beam as others. This is particularly notable in the x direction. This causes ridges that connect the rectangular pillars to each other. This can be better seen in an image taken by a metrology probe.

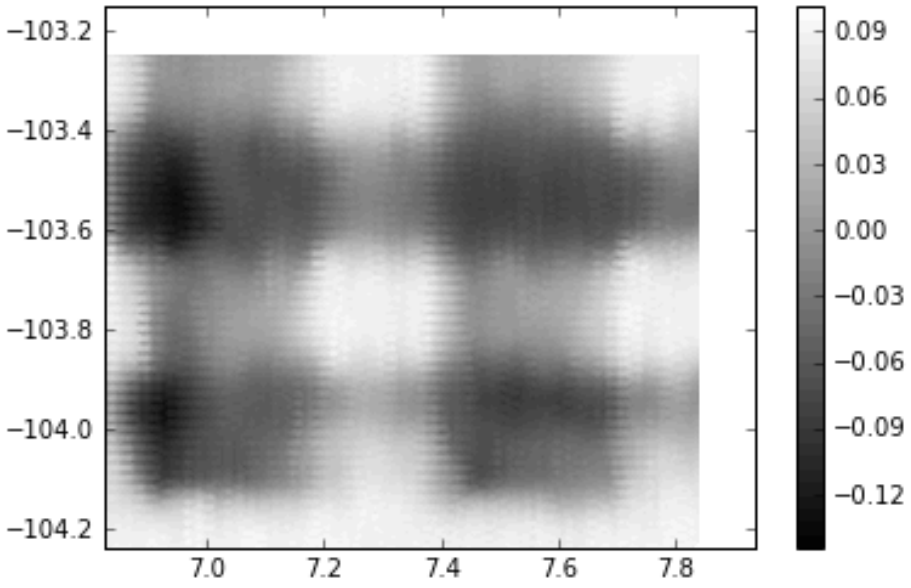

Figure 10: Feature image taken with confocal probe.

This image also gives us the ability to see the depth and size of our features. The depth of the trenches between the features is around 210 microns, the width of the trenches is around 200 microns, and the width of the pillars is also around 200 microns. An impressive aspect of these features is the cleanness of the edges of the cuts. These appear to vary at the sub-micron level, so we can be sure that we are cutting clean features into silicon.

We also tried ablating this pattern with alumina. We found the same redeposit difficulty with alumina, but again a water layer on the surface solved that problem.

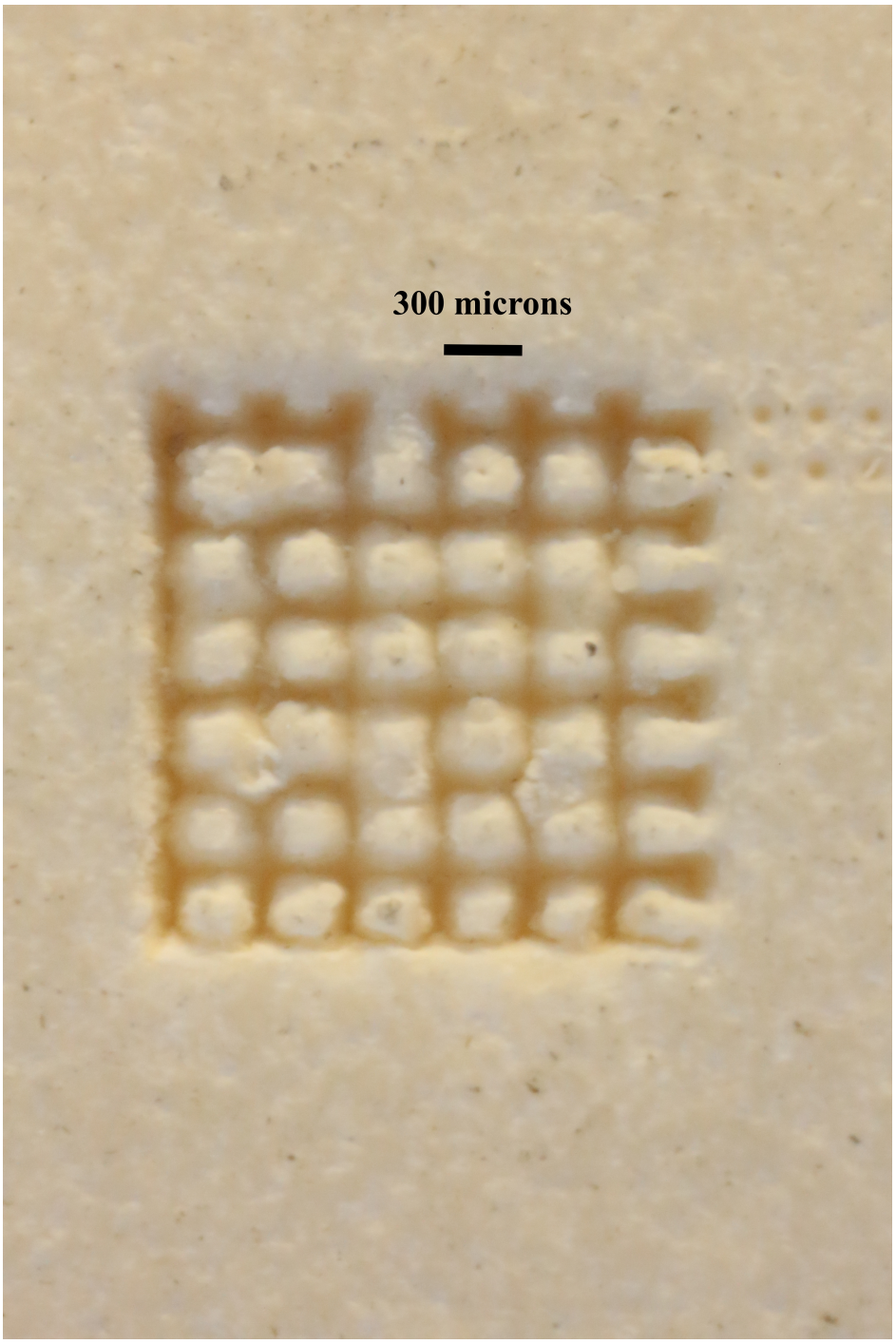

Figure 11: AR features in alumina.

A major issue that we have found with alumina is that the cuts we are making are not very clean like in silicon. This is still an ongoing issue and we hope that it can be resolved

simply by taking more passes over the same area.

6.2 Conical Geometry

We then turned to attempting the conical geometry in silicon. We machined this geometry by simply moving the beam to a point on the sample and then exposing the laser for a second or less. By just allowing the laser to naturally drill the cones with the beam's profile, we found that it made cones with a diameter of around 100 microns. To try and match our model, we then made a cone array with a pitch of 70 microns.

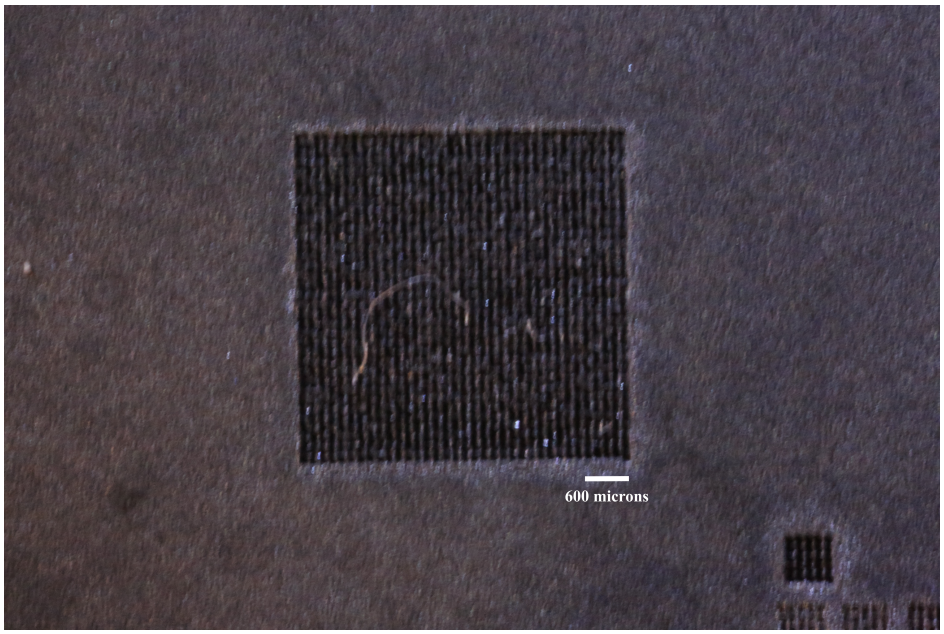

Figure 12: Conical array ablated onto silicon.

This image does not capture the depth of these cones very well, and we do not have any means to measure the depth because the pitch of these features is smaller than the resolution of our confocal probe. What this test showed is that it is possible to create a conical geometry with our current laser set-up. Further tests are being performed to create a sample that can have its reflectivity measured to see how it compares to the modeled

reflectance.

6.3 Cutting and Drilling

A more basic application of the laser machining system is the simple cutting and drilling of silicon wafers. This can be accomplished in a few different ways, two of which are summarized here.

A fortunate discovery occurred by accidentally allowing the water to evaporate while cutting the rectangular AR coating features. The result of arouind 100 passes without water was a square hole that had near vertical side walls.

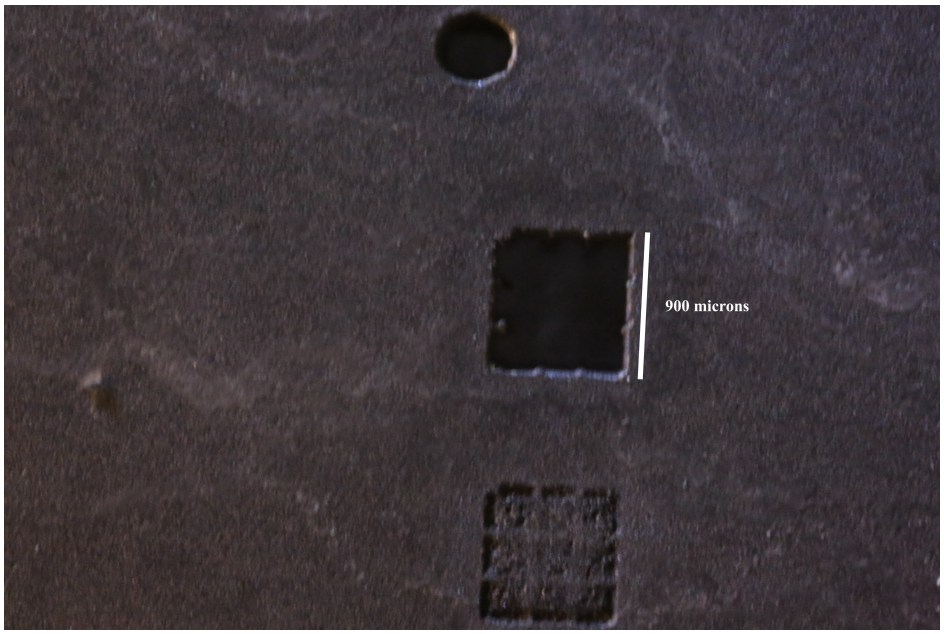

Figure 13: Square hole cut by laser.

This cutting can be used in the future for machining silicon wafers and then stacking those machined wafers to create three dimensional objects.

We can likewise drill holes by making a spiral and passing over the same area many times. This has likewise applications as the square holes, but also has a different application. If we stop the spiral cutting process before the material is ablated all the way through then we get a desired cone shape that is larger in diameter than the simple beam profile created cones. This allows us to potentially make cone arrays in different bands, or even more effective cone arrays in the modeled terahertz band.

7 Conclusions and Future Applications

We have found that the current experimental set up of laser machining is effective at creating desired features in silicon and alumina. The accuracy of our stages and optics are sufficient to create micron sized features accurately. We have also found that the general purpose of machining and drilling silicon is also possible with the current laser set up. Improvements can be made in the alumina regime and are being investigated. We would also like to make the cuts in silicon cleaner.

To improve the cuts in silicon a potential solution is to ablate the features in a chlorine gas environment. This has been found to speed up the process of ablation and well as improve the cleanness of the cuts. [9] This chemical etching process is currently being investigated and approached with caution due to the nature of the chemical etching. We will consider this process more fully if other attempts to improve the cuts in silicon fail.

With improvements, we should be able to machine optical facets of not only the ACT telescope, but also other experiments designed to operate in the frequency range of ACT. Furthermore, there is no reason that this technique should be limited to AR coatings. It is entirely plausible to machine stacked feed horn array by cutting and stacking wafers as previously described. [11] It is also possible, in the future, to apply the idea of using subwavelength features to create a quasi-index of refraction and create a flat lens by varying

the geometry of subwavelength features in a radial manner on a silicon wafer. If this is found to be plausible, the laser machining system described and summarized in this document would be ideal to create these features because of the degrees of freedom previously described. Again, if this is plausible and can be achieved with our set up, it could potentially open a new door in compact optical system design, which would be extremely useful in astrophysical observation.

8 Bibliography

References

[1] J.C. Mather et al. *Measurement of the Cosmic Microwave Background spectrum by the COBE FIRAS Instrument*. The Astrophysics Journal **420** 439-444. 1994 January 10.

[2] G.F. Smoot et al. *Structure in the COBE DMR First Year Maps*. Astrophysical Journal Letters. April 21, 1992.

[3] C.L. Bennet et al. *Nine-Year Wilkinson Microwave Anisotropy Probe (WMAP) Observations: Final Maps and Results*.

[4] J.W. Fowler et al. *The Atacama Cosmology Telescope: A Measurement of the 600< ℓ <8000 Cosmic Microwave Background Power Spectrum at 148 GHZ*. August 26, 2010.

[5] S.W. Henderson et al. *Advanced ACTPol Cryogenic Detector Arrays and Readout*. October 9, 2015.

[6] Spectra-Physics. *Talon Laser Systems: User's Manual*. Revision A. April 2015.

[7] R. Datta, C.D. Munson et al. *Large-Aperture Wide-Bandwidth Anti-Reflection-Coated Silicon Lenses for Millimeter Wavelengths*. July 17, 2013.

[8] T. Matsumura, K. Young, et al. *Millimeter-wave Broadband Antireflection Coatings Using Laser Ablation of Subwavelength Structures.* Applied Optics **55** 13. May 1, 2016.

[9] C. Drouet d'Aubigny. *Laser Chemical Etching of Waveguides and Quasi-Optical Devices.* May 2, 2003.

[10] P.A.R. Ade et al. *Joint Analysis of BICEP2/Keck Array and Planck Data.* Phys. Rev. Lett. **114** 101301. 2015

[11] J. Britton, K.W. Yoon et al. *Progress Toward Corrugated Feed Horn Arrays in Silicon*